Photo-induced antibacterial activity of a porphyrin derivative isolated from the harmful dinoflagellate *Heterocapsa circularisquama*

Li Wencheng[a], Kichul Cho[b], Yasuhiro Yamasaki[c], Satoshi Takeshita[d], Kiju Hwang[e], Daekyung Kim[e]*, Tatsuya Oda[a]*

[a]*Graduate School of Fisheries Science & Environmental Studies, Nagasaki University, 1-14 Bunkyo-machi, Nagasaki 852-8521, Japan*

[b]*Cell Factory Research Center, Korea Research Institute of Bioscience and Biotechnology (KRIBB), Daejeon, Republic of Korea*

[c]*Department of Applied Aquabiology, National Fisheries University, 2-7-1 Nagata-Honmachi, Shimonoseki, Yamaguchi 759-6595, Japan*

[d]*Joint Research Division, Center for Industry, University and Government Cooperation, Nagasaki University, 1-14 Bunkyo-machi, Nagasaki 852-8521, Japan*

[e]*Daegu Center, Korea Basic Science Institute (KBSI), Kyungpook National University, Daegu, Republic of Korea*

---

*Corresponding authors

TEL: +81-095-819-2831, FAX: +81-095-819-2831, E-mail: t-oda@nagasaki-u.ac.jp

TEL: +82-53-717-4312, FAX: +82-53-717-4329, E-mail: dkim@kbsi.re.kr

Abstract

The dinoflagellate *Heterocapsa circularisquama* is highly toxic to bivalves; however, significant toxicity to finfish species has not been reported. We previously found that *H. circularisquama* has light-dependent haemolytic agents. Purification and chemical structural analyses revealed that the haemolytic agent H2-a is a porphyrin derivative, which exhibits light-dependent cytotoxicity toward tumour cells. To clarify the biological activity of H2-a further, its antibacterial activities against Gram-positive and Gram-negative bacteria were investigated in this study. A fraction (F5) equivalent to H2-a purified from the methanol extract of *H. circularisquama* showed potent light-dependent bactericidal activity toward *Staphylococcus aureus*, and the activity was concentration- and light illumination time-dependent; however, *Escherichia coli* was highly resistant to F5. Electron microscopic observation suggested that F5 induces morphological changes in *S. aureus* in a light-dependent manner. Further analysis using other bacterial species showed that the Gram-positive bacterium *Bacillus subtilis* was more sensitive than the Gram-negative bacteria *Pseudomonas aeruginosa* and *Vibrio alginolyticus*. These results indicate that F5 is a photo-induced antibacterial agent with relatively higher specificity to Gram-positive bacteria. Iodometric assay suggested that singlet oxygen was generated from light illuminated F5. Histidine, a specific singlet oxygen scavenger, markedly inhibited the photosensitising antibacterial activity of F5 against *S. aureus*, suggesting the involvement of singlet oxygen in antibacterial activity. The antibacterial spectrum of F5 was evidently different from that of 5,10,15,20-tetra (*N*,*N*,*N*-trimethylanilinium) porphyrin tetratosylate, a commercially available porphyrin compound with antibacterial activity. Our results

demonstrate that *H. circularisquama* has a novel antibacterial photosensitiser, a porphyrin derivative, with relatively higher specificity to Gram-positive bacteria. To the best of our knowledge, this is the first study to discover a porphyrin derivative with antibacterial activity in marine microalga.

Keywords: *Heterocapsa circularisquama*; Harmful dinoflagellate; Porphyrin derivative; Antibacterial activity; Single oxygen; Photosensitising agent

1. Introduction

Heterocapsa circularisquama is one of the most noxious dinoflagellates causing harmful algal blooms (HABs) in Japan (Horiguchi, 1995; Matsuyama et al., 1996). HABs due to *H. circularisquama* occurred for the first time in Uranouchi Bay in southern Shikoku Island in 1988 and caused mass mortality (more than 1500 tons) of the short-necked clam *Ruditapes philippinarum* (Matsuyama et al., 1996). In the next year, *H. circularisquama* bloom occurred in Fukuoka Bay, northern Kyushu Island, and caused mass mortality of bivalve molluscs (Yamamoto and Tanaka, 1990). Since then, *H. circularisquama* has been continuously causing HABs leading to bivalve mortality in several localities in western Japan, and in 2009, it expanded to Niigata Prefecture, an eastern area in Japan, where it caused the mortality of bivalves (Kondo et al., 2012). Although the incidence of HABs of *H. circularisquama* associated with mass mortality of shellfish decreased during the 2000–2008 period, it seems to be on a course of revival since 2009 (Basti et al., 2016). Recent studies found that *H.*

70 *circularisquama* can also damage the early developmental stages of bivalves (Basti et
71 al., 2013). Although the potent lethal effects of *H. circularisquama* on pearl oyster
72 (*Pinctada fucata*), short-necked clam (*R. philippinarum*), and oyster (*Crassostrea*
73 *gigas*) have been reported, its harmful effects on wild and cultured finfish and other
74 marine vertebrates have not been reported so far (Matsuyama et al., 1992; Yamamoto
75 and Tanaka, 1990).

76 In addition to bivalves, *H. circularisquama* exhibits lethal effects on the
77 microzooplankton tintinnid ciliate *Favella taraikaensis* (Kamiyama, 1997; Kamiyama
78 and Arima, 1997) and rotifer (*Brachionus plicatilis*) (Kim et al., 2000) in a cell
79 density-dependent manner. Frequent contact of these microzooplanktons with *H.*
80 *circularisquama* can induce detrimental effects. Furthermore, it has been reported that
81 *H. circularisquama* showed cell contact-dependent toxicity on other phytoplankton
82 species (Yamasaki et al., 2011).

83 Matsuyama (2012) proposed that live *H. circularisquama* cell-mediated
84 direct contact with bivalves is essential for exerting lethal effects, and certain toxins
85 located on the cell surface might play an important role in this regard. However, the
86 isolation and characterisation of such toxins from the organism has not yet been
87 successful, probably due to the extremely unstable nature of the supposed toxins of *H.*
88 *circularisquama* (Matsuyama, 2012).

89 We previously found that *H. circularisquama* cell suspension caused potent
90 haemolysis of rabbit erythrocytes when erythrocytes were directly exposed to the
91 dinoflagellate cells (Oda et al., 2001). The cell-free culture supernatant prepared from
92 the live cell suspension of *H. circularisquama* also showed haemolytic activity, but at a
93 much lower level, suggesting that only a small part of the haemolytic toxin might have

been discharged from the cells into the culture medium (Oda et al., 2001; Sato et al., 2002). We also found that the haemolytic activities of different strains of *H. circularisquama* isolated from different localities in Japan were different, and the differences in activities were well correlated with the differences in their toxicity towards shellfish (Kim et al., 2002). These findings suggest that haemolytic toxins, which are probably located on the cell surface of *H. circularisquama*, might play an important role in shellfish killing. Pathological studies of Mediterranean mussel (*Mytilus galloprovincialis*) exposed to *H. circularisquama* demonstrated that the most affected organ was the gill, followed by the labial palps and mantle, the stomach and intestine, and the hepatopancreas (Basti et al., 2015).

Some phytoplankters produce multiple toxins and some of these toxins exhibit haemolytic activity. For instance, palytoxin (Habermann et al., 1989) and maitotoxin (Igarashi et al., 1999) are known to induce Ca^{2+} influx into mammalian erythrocytes and subsequently cause haemolysis. We previously found that an ethanol extract prepared from *H. circularisquama* showed light-dependent haemolytic activity (Oda et al., 2001; Sato et al., 2002). Purification and characterisation studies suggested that a photosensitising haemolytic agent, H2-a, has structural similarity to pyropheophorbide *a* methyl ester, a well-known photosensitising haemolytic agent (Miyazaki et al., 2005). Comparative studies on the cytotoxicity of H2-a and pyropheophorbide *a* methyl ester to human cervical cancer cells (HeLa cells) suggested that H2-a induces necrotic cell death, whereas pyropheophorbide *a* methyl ester triggers apoptosis (Kim et al., 2008). Although the exact reason for the difference in type of cell death induced is still unclear, it is speculated that the relatively high affinity of H2-a to the plasma membrane might result in quick membrane damage,

leading to the collapse of targeted cells without induction of apoptotic intracellular signal transduction (Kim et al., 2008).

On the other hand, porphyrin derivatives have been used for photodynamic therapy, and there are numerous their applications including inactivation of pathogens and treatments of protozoa diseases (8 T.N.Demidova,), bacterial, fungal and viral infections (9 G.B. Kharkwal), and cancer (10 P. Agostinis). For example, it has been reported that pheophorbide *a* causes apoptotic cell death of *Leishmania amazonesis*, a causative organism of Leishmaniasis (Miranda *et al.* 2017).

Our recent studies found that *H. circularisquama* exhibits antibacterial activity in dinoflagellate/bacteria co-culture system to different extents depending on the bacterial species (Cho et al., 2017). Detailed analyses suggested that *H. circularisquama* has two different types of antibacterial agents. One is located on the cell surface and is mainly responsible for dinoflagellate cell-mediated bactericidal activity. The other one is an intracellular agent that can be discharged from ruptured *H. circularisquama*. Notably, intracellular agents showed light-dependent antibacterial activity towards *S. aureus*, while no such activity was detected against *Escherichia coli* (Cho et al., 2017). It is most likely that intracellular light-dependent antibacterial agents are porphyrin derivatives that we previously identified as light-dependent haemolytic and cytotoxic agents as described above. However, there is no available information about porphyrin derivatives with antibacterial activity discovered in the marine microalga so far. To clarify this point, we isolated the porphyrin derivative from *H. circularisquama* by previously reported methods and conducted detailed examinations on its antibacterial activities against various bacterial strains. Our studies may provide not only a new insight into biochemical characterization of porphyrin

142 derivative as potential toxic agent of *H. circularisquama* but also a possibility for its
143 usefulness as new antibacterial agent.
144
145 **2. Materials and Methods**
146
147 *2.1. Plankton culture*
148
149 *H. circularisquama*, which was originally isolated from Ago Bay, Japan in
150 1994 (Matsuyama, 1999), was kindly provided by Dr. Y. Matsuyama (Seikai National
151 Fisheries Research Institute, Japan) in 2000. Since then, the strain has been maintained
152 in our laboratory under the conditions described below. The plankton culture was
153 maintained at 26°C in a 100 mL flask containing 60 mL of a modified seawater
154 medium (SWM3) at a salinity of 25 (Yamasaki et al., 2007) in a 12:12 h photoperiod
155 using a cool-white fluorescent lamp (150 ± 5 μmol m^{-2} s^{-1}). The modified SWM3
156 contained a Tris-HCl buffer system and was autoclaved for 15 min at 121°C before use.
157 The cell number of the culture was counted microscopically using a haemocytometer
158 (Erma Inc., Tokyo, Japan).
159
160 *2.2. Bacterial cultures*
161
162 *S. aureus* (NBRC12732), *E. coli* (NBRC13898), *Vibrio alginolyticus* (NBRC15630),
163 and *Pseudomonas aeruginosa* (IFO3445) were obtained from NITE Biological Resource
164 Centre (Tsukuba, Japan). *Bacillus subtilis* (ATCC6633) was obtained from American
165 Type Culture Collection (Rockville, MD, USA). Nutrient agar (for *S. aureus*, *E. coli*, *B.*

166 *subtilis*, and *P. aeruginosa*) and Zobell marine agar (for *V. alginolyticus*) were used to
167 maintain the strains. Bacterial strains were cultured 18 h at 34°C in nutrient broth (for *S.*
168 *aureus*, *E. coli*, *B. subtilis*, and *P. aeruginosa*) or in Zobell marine medium (for *V.*
169 *alginolyticus*). Then, the cells were harvested and washed with phosphate-buffered
170 saline (PBS) by centrifugation at 15,000 × *g* for 10 min at 4°C. The final cell pellets
171 were diluted to the appropriate cell density with PBS and immediately used for the
172 experiments. Practical salinity unit (pus) of nutrient broth and Zobell marine medium
173 used in this study were 7 and 35, respectively.
174
175 *2.3. Preparation of methanol extract*
176
177 Methanol extract was prepared from *H. circularisquama* in its late exponential
178 growth phase as described previously (Miyazaki et al., 2005). In brief, the cell pellets
179 prepared from 2 L of cultured *H. circularisquama* (2×10^8 cells L^{-1}) by centrifugation
180 (5000 x *g* for 10 min at 4°C) was resuspended in 10 mL of methanol and vigorously
181 agitated by sonication at 25°C. After centrifugation at 15,000 × *g* for 10 min at 4°C, the
182 supernatant was collected and stored at -30°C until use as the methanol extract.
183
184 *2.4. Purification of antibacterial agent from methanol extract*
185
186 Purification of antibacterial agent from methanol extract prepared from *H.*
187 *circularisquama* was conducted by a column chromatography using Sephadex LH-20.
188 The pooled methanol extract prepared from 20 L of *H. circularisquama* culture was
189 applied to a Sephadex LH-20 column (3 x 45 cm; Pharmacia, Uppsala, Sweden), which

was previously equilibrated with methanol by the elution with enough amount of methanol. The extract was applied to the column, and then eluted with methanol continuously. The elution profile was monitored at 450 nm. Based on the elution profile, six fractions (F1–F6) were obtained (Fig. 1). To check the purity of the separated fractions, each fraction was concentrated by evaporation, subjected to silica gel thin-layer chromatography (TLC), and developed with a developing solvent mixture of chloroform and methanol at a ratio of 60:10 (v/v). The spots on the silica gel thin-layer coated with flourescent indicator were detected under ultra violet irradiation. The antibacterial activity of each fraction against *S. aureus* was measured by colony formation assay as described below.

2.5. Measurement of antibacterial activity

Samples prepared from methanol extract of *H. circularisquama* was appropriately diluted with PBS and added to each bacterial cell suspension in PBS in 0.5–1.5 mL of total assay mixture. After incubation for 0.5~2 h in the light (400 ± 5 μmol m^{-2} s^{-1}) or in the dark at 26°C, 10–50 μL aliquots of the bacterial cell suspension treated with the samples (reaction mixture) were withdrawn for the enumeration of viable bacteria. An aliquot of each reaction mixture was suitably diluted with PBS and inoculated in triplicates into nutrient agar medium (for *S. aureus*, *E. coli*, *B. subtilis*, and *P. aeruginosa*) or Zobell marine agar medium (for *V. alginolyticus*). After 18 h of incubation at 37°C in the dark, the number of colonies formed was counted (colony forming unit; CFU).

2.6. Electron microscopy

Cell suspensions of pure cultures of *S. aureus* and *E. coli* from photosensitising antibacterial experiments were processed for electron microscopic observations according to the procedures reported previously (Laue and Bannert, 2010). In brief, 5 µL of cell suspension in PBS was placed on grids coated with plastic-carbon support film and incubated for 30 min under ultraviolet (UV) illumination. After washing four times with double-distilled water, the cells were stained with 0.5% uranyl acetate and then dried. Finally, the cells were observed with a Hitachi H-7100 transmission electron microscope (accelerating voltage, 100kV) equipped with an Olympus Megaview G2 TEM CCD camera.

2.7. Estimation of membrane damage

Intracellular macromolecules especially DNA and RNA have absorbance at 260 nm, and these molecules are released into the culture medium during cellular damage or loss of membrane integrity (Frontiers in Microbiology, 2016, vol. 7 article 242,p1~8). The extent of membrane damage was estimated by an increase in absorbance at 260 nm. The bacterial cells (5 x 10^8 cells mL^{-1} in PBS) were treated with 20 µg mL^{-1} F5 for 2 h in the dark or in the light (400 ± 5 µmol m^{-2} s^{-1}) at 26°C. After centrifugation (15,000 × *g* for 10 min at 4°C), the absorbance of the supernatant at 260 nm was measured.

2.8. Binding assay to bacterial cells

238

239 Purified porphyrin sample was added to *S. aureus* or *E. coli* cell suspension in
240 PBS (5 x 10^8 CFU mL^{-1}) at a final concentration of 2.2 μg mL^{-1}. After incubation at
241 26°C for 0, 15, 30, and 60 min in the dark, an aliquot of the assay mixture was
242 withdrawn, and the cells were centrifuged for 10 min at 15,000 × *g* at 4°C. Fluorescent
243 intensity of the supernatant was measured at excitation and emission wavelengths of
244 460 and 530 nm, respectively. Meanwhile, the pelleted cells obtained after 60 min
245 incubation were resuspended in PBS and washed with PBS by centrifugation (15,000 ×
246 *g* for 10 min at 4°C). The final cell pellet was suspended in 1 mL PBS containing 2%
247 sodium dodecyl sulphate (SDS) and incubated at room temperature for 30 min. After
248 centrifugation (15,000 × *g* for 10 min at 4°C), fluorescent intensity of the supernatant
249 was measured as described above. The cell pellets were also treated with dimethyl
250 sulfoxide (DMSO) at room temperature and sonicated. The mixtures were centrifuged
251 (15,000 × *g* for 10 min at 4°C), and the DMSO supernatants were obtained for
252 fluorescence measurement as described above. The concentration of F5 was estimated
253 based on the standard curves of fluorescence intensity versus concentration of F5 in 2%
254 SDS in PBS or DMSO.

255

256 *2.9. Detection of singlet oxygen*

257

258 The production of singlet oxygen was measured by an iodometric method (Cerny
259 et al., 2010). The singlet oxygen specifically reacts with iodide reagent to produce
260 triiodide (I_3^-), which can be detected spectrophotometrically by measuring the
261 absorbance at 355 nm. Samples in PBS (final 2 μg mL^{-1}) were incubated under the same

conditions (illumination or darkness and temperature) as the antibacterial experiments. Changes in absorbance at 355 nm were monitored during the 4-h incubation period. To examine the effects of histidine on singlet oxygen production, F5 in PBS (final 2 μg mL^{-1}) was incubated in the presence of histidine (final 20 mM) under illumination conditions as described above. After 4 h, an increase in absorbance at 355 nm was observed.

2.10. Statistical analysis

All the experiments were performed in triplicate and data were expressed as the mean ± standard deviation. Data were analysed with a paired Student's *t*-test to evaluate significant differences. $P < 0.05$ was considered statistically significant.

3. Results and Discussion

3.1. Isolation of porphyrin derivative with antibacterial activity from H. circularisquama

In our previous studies, we found that photosensitising haemolytic toxins were efficiently extracted into alcohol (Sato et al., 2002), and the resulting alcohol extract contained at least three isoforms of haemolytic compounds (Miyazaki et al., 2005). Among these compounds, H2-a, a highly purified one, was the most abundant haemolytic agent, and it was cytotoxic as well (Miyazaki et al., 2005; Kim et al., 2008). Chemical structural analysis revealed that H2-a is a porphyrin derivative with a

286 structure similar to pyropheophorbide *a* methyl ester, a known light-dependent
287 haemolytic agent (Miyazaki et al., 2005). According to the purification procedure of
288 H2-a, in this study, methanol extract was prepared from *H. circularisquama*, and the
289 extract was applied to a Sephadex LH-20 column. Based on the elution profile (Fig.
290 1A), six fractions (F1–F6) were obtained. Each pooled fraction was diluted with PBS
291 and adjusted to final concentration of 0.01% (v/v), and then the antibacterial activity
292 against *S. aureus* was examined. Methanol in PBS at 0.01% had no antibacterial
293 activity against *S. aureus* (data not shown). As shown in Figure 1B, only F5 equivalent
294 to H2-a showed antibacterial activity. TLC analysis (Fig. 1C) showed that F5 exhibited
295 a single spot, which has almost equal retention factor (Rf) value to H2-a (Miyazaki et
296 al., 2005), Even under ultra violet irradiation, no other spots were detected. These
297 results suggest that a main ingredient in F5 is H2-a. The absorption spectrum of F5
298 (Fig. 1D) was also quite similar to that of H2-a (Miyazaki et al., 2005). These results
299 suggest that F5 mainly contains H2-a. Detailed analysis of the antibacterial activity of
300 F5 against *S. aureus* demonstrated that the activity was concentration- and light
301 exposure time-dependent (Fig. 2). In contrast, *E. coli* was highly resistant to F5, and
302 only a slight decrease in CFU was observed even at the highest concentration of F5 (20
303 μg mL^{-1}) after 2 h incubation at 26°C in the light (Fig. 2). One possible explanation for
304 this result is the different organization of the cell wall between Gram-negative and
305 -positive bacteria. The presence of outer membrane and relatively wide periplasmic
306 space makes Gram-negative bacteria more resistant to the photosensitising bactericidal
307 activity of porphyrins, including F5, than Gram-positive bacteria (Lazzeri et al., 2004).
308 To clarify this point further and to evaluate the antimicrobial spectrum of F5, the
309 antibacterial activities of F5 against *B. subtilis*, *P. aeruginosa*, and *V. alginolyticus* in

addition to *S. aureus* and *E. coli* were investigated. *V. alginolyticus* is a typical marine bacterium and grows well in medium with high salinity, while other bacteria are sort of fresh water or terrestrial bacteria, which grow in nutrient medium with normal salinity. The activities were compared with those of the commercially available porphyrin derivative, 5,10,15,20-tetra(*N*,*N*,*N*-trimethylanilinium)porphyrin tetratosylate (TPT), which has been reported to have photosensitising bactericidal activity (Banfi et al., 2006). As shown in Figure 3A, the Gram-positive bacterium *B. subtilis* was more sensitive to F5 than *S. aureus*, and these Gram-positive bacteria tended to be much more sensitive to F5 than Gram-negative bacteria. Similar to *E. coli*, Gram-negative marine bacterium *V. alginolyticus* also showed resistance to F5, and more than 50% of the bacteria survived at a concentration of 20 μg/mL after 2 h at 26°C (inset of Fig. 3A). Based on these results, the sensitivities of bacteria to F5 were in the order: *B. subtilis* > *S. aureus* > *P. aeruginosa* > *E. coli* = *V. alginolyticus*. The antibacterial spectrum of F5 was noticeably different from that of the commercial porphyrin tested (Fig. 3B). Our results suggest that susceptibilities of these bacteria to F5 and TPT were significantly different depending on the species. Despite of the fact that *E. coli* was resistant to both F5 and TPT, *V. alginolyticus* was highly sensitive to TPT, but quite resistant to F5, whereas *P. aeruginosa* was relatively sensitive to F5, but resistant to TPT. In the case of Gram positive bacteria, TPT was less effective to *B. subtilis* than F5, although *S. aureus* was almost equally sensitive to F5 and TPT. Although the exact reason for the different antibacterial spectra of F5 and TPT is still unclear, there may be some bacterial species resistant to F5 but sensitive to TPT, and vice versa. When it comes to practical application

of F5 as an antibacterial therapeutic agent, the antibacterial spectrum of F5 can provide useful information. Obviously further studies using wide variably of bacterial species are necessary to evaluate the potentiality of F5 as a therapeutic agent.

The antibacterial activities of both F5 and TPT were absolutely light-dependent, and no significant activities against *E. coli* and *S. aureus* were observed even after 8 h of incubation in the dark (Fig. 4). These results suggest that F5 may be a novel porphyrin derivative with antibacterial activity. Bioactivities, including antibacterial activities, of naturally occurring and synthetic porphyrin derivatives have been widely studied (Soukos et al., 1998; Hamblin and Hasan, 2004). It has been demonstrated that the chemical structural elements deeply influence bioactivities, and cationic porphyrins are more active than anionic or non-ionic derivatives against both Gram-positive and Gram-negative bacteria (Merchat et al. 1996). Since chemical modification of porphyrin structure can lead to the production of more efficient and appropriate photosensitising antibacterial agents (Banfi et al., 2006), F5 may be used as a precursor for such agents. Further studies are required to verify such possibility.

Although ecological rationale or biological significance of F5 especially during HAB due to *H. circularisquama* is still unclear, our previous studies demonstrated that intracellular haemolytic agent of *H. circularisquama* exhibits harmful effects on surrounding microalgae including *H. circularisquama* cells themselves and micro zooplankton rotifer (Nishiguchi et al 2016). Hence, one can speculate that intracellular toxic agents present in F5 can impact on multiple microorganisms. Further studies are necessary to clarify these points.

3.2. Morphological changes of bacterial cells

The effect of F5 on bacterial cell morphology was investigated by transmission electron microscopy (TEM). The representative TEM micrographs are shown in Figure 5. The rod-like morphology of *E. coli* and round morphology of *S. aureus* were observed in untreated control (Fig. 5A and B). No significant morphological changes were observed in both the bacterial strains treated with F5 in the dark (Fig. 5C and D). In *S. aureus* treated with F5 under light illumination, the bacterial structure was damaged (Fig. 5F), whereas no significant cell structural damage was induced in *E. coli* treated under the same conditions (Fig. 5E). These results were consistent with the photosensitising antibacterial activities of F5 (Fig. 2), and it is obvious that F5 could specifically damage *S. aureus* cell wall and membrane in a photosensitising manner.

Cellular damage or loss of membrane integrity often leads to release of intracellular macromolecules, such as DNA and RNA, which have specific absorbance at 260 nm. Hence, the measurement of absorbance at 260 nm can be used to estimate membrane damage (Xu, et al. 2016). As shown in Figure 6, under light illumination, a significant increase in absorbance of the supernatant of F5-treated *S. aureus* at 260 nm was observed, whereas the increase was much lower in *E. coli*. The values obtained in the dark were comparable to that in the control without F5. These results suggest that F5 specifically damaged the cells of *S. aureus* in a light-dependent manner, but not *E. coli* cells.

3.3. Binding of F5 to bacterial cells

382 Several factors are considered to contribute to the toxic action of F5 to bacteria.
383 The ability of F5 to bind to the bacterial cells may be the most important factor. It has
384 previously been reported that the low sensitivity of Gram-negative bacteria to anionic
385 porphyrin-related compounds is due to the lack of binding of the compounds to the
386 bacterial membrane (Minnock et al., 1996). To evaluate whether the differences in
387 susceptibility of *S. aureus* and *E. coli* to F5 could be due to the difference in binding of
388 F5 to these bacterial strains, a binding assay was conducted based on the intrinsic
389 fluorescence property of F5. In both *S. aureus* and *E. coli* cell suspensions incubated
390 with F5 (final 2.2 μg mL^{-1}), the levels of F5 found in the supernatant gradually
391 decreased and reached to 2.3 and 11.3% of the initial levels after 60 min, respectively.
392 However, the rate of F5 decrease in the supernatant of *S. aureus* was higher than that of
393 *E. coli* during the first 30 min (Fig. 7A). These results indicate that F5 is capable of
394 binding to both bacterial strains, but F5 may have a slightly higher affinity to *S. aureus*
395 than *E. coli*. Reflecting the decrease in amounts of F5 in the supernatants,
396 approximately 60 and 50% of F5 was recovered by SDS treatment from *S. aureus* and
397 *E. coli* cells incubated for 60 min, respectively (Fig. 7B). The remaining F5 was
398 recovered by DMSO extraction, and 95 and 92% of F5 were detected in DMSO
399 extracts of *S. aureus* and *E. coli* cell pellets, respectively. Differences between SDS
400 and DMSO treatment may be due to the location of F5 in the cells. Although F5 bound
401 on the bacterial cell surface can be easily recovered by SDS treatment, DMSO
402 treatment may be necessary for the recovery of more tightly bound or intracellularly
403 incorporated F5. The differences in binding affinity of F5 to the bacterial cells may be
404 insufficient to explain the differences in susceptibility of *S. aureus* and *E. coli*, and the
405 pattern or location of binding of F5 may be more important for the activity of F5.

406

407 *3.4. Generation of singlet oxygen*

408

409 Although the exact photosensitising antibacterial mechanisms of porphyrin
410 derivatives have not been fully clarified yet, singlet oxygen ($^1O_2$), which can be
411 generated through energy transfer from excited state to oxygen (O_2), is thought to play
412 a key role in antibacterial activity (Henderson and Daugherty, 1992). To ascertain this
413 point, the kinetics of singlet oxygen production in F5 solution was measured by
414 iodometric method under the same conditions used for antibacterial assay. As shown in
415 Figure 8, almost linear increase in the absorbance at 355 nm was observed in F5
416 solution under light illumination, reflecting singlet oxygen formation. The addition of
417 histidine (final 20 mM), a specific singlet oxygen scavenger, significantly reduced the
418 increase in absorbance. In the dark, the absorbance of F5 solution remained at the
419 initial level throughout the incubation period. These results suggest that F5 is capable
420 of generating singlet oxygen upon light activation.

421 It has been reported that photosensitisers, such as porphyrins, can modify many
422 biological molecules through the generation of reactive oxygen species (ROS)
423 including singlet oxygen, and eventually lead to cell death (Moan and Peng, 2003). To
424 assess the involvement of singlet oxygen in the photosensitising antibacterial activity
425 of F5, the effects of various concentrations of histidine on the photosensitising
426 antibacterial activity of F5 against *S. aureus* were examined. As expected, histidine
427 showed a significant inhibitory effect on F5 toxicity in a concentration-dependent
428 manner (Fig. 9). These results suggest that singlet oxygen generated by photoactivated
429 F5 plays an important role in antibacterial activity.

Electron spin resonance (ESR) is generally known to be the most reliable method to detect reactive oxygen species. ESR spectroscopy with the specific spin traps can detect singlet oxygen, superoxide anion, and hydroxyl radical individually, and the characteristic ESR spectra are obtained depending the reactive oxygen species. In fact, a detail ESR analysis demonstrated that a certain cationic porphyrin produced superoxide anion and hydroxyl radical in addition to singlet oxygen, and it is considered that these reactive oxygen species are differently involved in the antibacterial activity (Solar Energy 82, 2008, 1107-1117 Karim Ergaieg et al). In the case of F5, ESR analysis may also be necessary to confirm the generation of singlet oxygen and other reactive oxygen species (ROS). ROS are generally know to be highly reactive and can damage various cellular molecules such as proteins, nucleic acids, and lipids, leading to cytotoxicity. Due to the multiple targets, it is considered that bacteria can hardly acquire the resistance mechanism (Tavares et al., 2010). Hence, porphyrin derivatives including F5 with ROS-mediated toxic actin mechanism may be useful as therapeutic agents against antibiotic resistance bacterial species such as methicillin-resistant *S. aureus* (MRSA).

4. Conclusions

The porphyrin derivative (F5) isolated from the harmful dinoflagellate *H. circularisquama* showed potent photosensitising antibacterial activity with relatively higher specificity to Gram-positive bacteria. An iodometric assay revealed that singlet oxygen was generated from photoactivated F5. Moreover, the antibacterial activity of F5 was significantly inhibited by histidine, a specific singlet oxygen scavenger,

454 suggesting that singlet oxygen is a major factor responsible for the antibacterial activity
455 of F5. To our knowledge, this is the first report to discover a porphyrin derivative with
456 antibacterial activity in a marine microalga.
457
458 **Acknowledgements**
459
460 This work was supported in part by a Grant-in-Aid (15K07580) for Scientific Research
461 from the Ministry of Education, Culture, Sports, Science and Technology of Japan,
462 This work was also supported by Korea Basic Science Institute (C38230) partly and the
463 National Research Foundation of Korea (NRF-2017R1A2B4005582).
464
465 **References**
466
467 Banfi, S., Caruso, E., Buccafurni, L., Battini, V., Zazzaron, S., Barbieri, P., Orlandi, V.,
468 2006. Antibacterial activity of tetraaryl-porphyrin photosensitizers: an in vitro
469 study on Gram negative and Gram positive bacteria, *J. Photoch. Photobio. B.,* 85,
470 28–38.
471 Basti, L., Nagai, K., Tanaka, Y., Segawa, S., 2013. Sensitivity of gametes, fertilization,
472 and embryo development of the Japanese pearl oyster, *Pinctada fucata martensii*, to
473 the harmful dinoflagellate, *Heterocapsa circularisquama*. *Mar. Biol.*, 160(1),
474 211–219.
475 Basti, L., Endo, M., Segawa, S., Shumway, S.E., Tanaka, Y., Nagai, S., 2015.
476 Prevalence and intensity of pathologies induced by the toxic dinoflagellate,

Heterocapsa circularisquama, in the Mediterranean mussel, *Mytilus galloprovincialis*. *Aquat. Toxicol.*, 163, 37–50.

Basti, L., Nagai, S., Watanabe, S., Oda, T., Tanaka, Y., 2016. Neuroenzymatic activity and physiological energetics in Manila clam, *Ruditapes philippinarum*, during short-term sublethal exposure to harmful alga, *Heterocapsa circularisquama*. *Aquat. Toxicol.*, 176, 76–87.

Cerny, J., Karaskova, M., Rakusan, J., Nespurek, S., 2010. Reactive oxygen species produced by irradiation of some phthalocyanine derivatives. *J. Photochem. Photobiol. A-Chem.*, 210, 82–88.

Cho, K., Wencheng, L., Takeshita, S., Seo, J.K., Chung, Y.H., Kim, D., Oda, T., 2017. Evidence for the presence of cell-surface bound and intracellular bactericidal toxins in the dinoflagellate *Heterocapsa circularisquama*. *Aquat. Toxicol.*, 189, 209–215.

Habermann, E., Hudel, M., Dauzenroth, M.E., 1989. Palytoxin promotes potassium outflow from erythrocytes, HeLa and bovine adrenomedullary cells through its interaction with Na^+, K^+ -ATPase. *Toxicon*, 27, 419–430.

Hamblin, M.R., Hasan, T., 2004. Photodynamic therapy: a new antimicrobial approach to infectious disease?. *Photochem. Photobiol. Sci.*, 3, 436–450.

Henderson, B.W., Dougherty, T.J., 1992. How does photodynamic therapy work?. *Photochem. Photobiol.*, 55, 145–157.

Horiguchi, T., 1995. *Heterocapsa circularisquama* sp. nov. (Peridiniales. Dinophyceae): a new marine dinoflagellate causing mass mortality of bivalves in Japan. *Phycol. Res.*, 43, 129–136.

Igarashi, T., Aritake, S., Yasumoto, T., 1999. Mechanisms underlying the hemolytic

501 and ichthyotoxin activities of maitotoxin. *Nat. Tox.*, 7, 71–79.
502 Kamiyama, T., 1997. Growth and grazing respones of tintinnid ciliates feeding on the
503 toxic dinoflagellate *Heterocapsa circularisquama*. *Mar. Biol.*, 128, 509–515.
504 Kamiyama, T., Arima, S., 1997. Lethal effect of the dinoflagellate *Heterocapsa*
505 *circularisquama* upon the tintinnid ciliate *Favella taraikaensis*. *Mar. Ecol. Prog.*
506 *Ser.*, 160, 27–33.
507 Kim, D., Sato, Y., Oda, T., Muramatsu, T., Matsuyama, Y., Honjo, T., 2000. Specific
508 toxic effect of *Heterocapsa circularisquama* dinoflagellate on the rotifer
509 *Brachionus plicatilis*. *Biosci. Biotechnol. Biochem.*, 64, 2719–2722.
510 Kim, D., Sato, Y., Miyazaki, Y., Oda, T., Muramatsu, T., Matsuyama, Y., Honjo, T.,
511 2002. Comparison of hemolytic activities among strains of *Heterocapsa*
512 *circularisquama* isolated in various localities in Japan. *Biosci. Biotechnol.*
513 *Biochem.*, 66, 453–457.
514 Kim, D., Miyazaki, Y., Nakashima, T., Iwashita, T., Fujita, T., Yamaguchi, K., Choi,
515 K.S., Oda, T., 2008. Cytotoxic action mode of a novel porphyrin derivative
516 isolated from harmful red tide dinoflagellate *Heterocapsa circularisquama*. *J.*
517 *Biochem. Mol. Toxicol.*, 22, 158–165.
518 Kondo, S., Nakao, R., Iwataki, M., Sakamoto, S., Itakura, S., Matsuyama, Y., Nagasaki,
519 K., 2012. Heterocapsa circularisquama coming up north? Mass mortality of
520 Pacific oysters due to its blooming at Lake Kamo in Sado Island, *Japan. Nippon*
521 *Suisan Gakkaishi*, 78, 719–725 (in Japanese with English abstract).
522 Laue, M., Bannert, N., 2010. Detection limit of negative staining electron microscopy
523 for the diagnosis of bioterrorism-related micro-organisms. *J. Appl. Microbiol.*,
524 109, 1159–1168.

525 Lazzeri, D., Rovera, M., Pascual, L., Durantini, E., 2004. Photodynamic studies and
526 photoinactivation of *Escherichia coli* using meso-substituted cationic porphyrin
527 derivatives with asymmetric charge distribution. *Photochem. Photobiol.,* 80,
528 286–293.
529 Matsuyama, Y., Nagai, K., Mizuguchi, T., Fujiwara, M., Ishimura, M., Yamaguchi, M.,
530 Uchida, T., Honjo, T., 1992. Ecological features and mass mortality of pearl
531 oysters during red tide of *Heterocapsa* sp. in Ago Bay in 1992. *Nippon Suisan*
532 *Gakk.*, 61, 35–41.
533 Matsuyama, Y., Uchida, T., Nagai, K., Ishimura, M., Nishimura, A., Yamaguchi, M.,
534 Honjo, T., 1996. Biological and environmental aspects of noxious dinoflagellate
535 red tides by *Heterocapsa circularisquama* in the west Japan. In: Yasumoto, T.,
536 Oshima, Y., Fukuyo, Y. (Eds.), Harmful and toxic algal blooms.
537 Intergovernmental Oceanographic Commission of UNESCO. pp. 247–250.
538 Matsuyama, Y., 1999. The toxic effects of *Heterocapsa circularisquama* on bivalve
539 molluscs. *Bull. Plank. Soc. Jpn.*, 46, 157–160.
540 Matsuyama, Y., 2012. Impacts of the harmful dinoflagellate *Heretocapsa*
541 *circularisquama* bloom on shellfish aquaculture in Japan and some experimental
542 studies on invertebrates. *Harmful algae*, 14, 144–155.
543 Merchat, M., Spikes, J.D., Bertoloni, G., Jori, G., 1996. Studies on the mechanism of
544 bacteria photosensitization by meso-substituted cationic porphyrins. *J.*
545 *Photochem. Photobiol. B: Biol*., 35, 149–157.
546 Minnock, A., Vernon, D.I., Schofield, J., Griffiths, J., Parish, J.H., Brown, S.B., 1996.
547 Photoinactivation of bacteria. Use of a cationic water-soluble zinc
548 phthalocyanine to photoinactivate both Gram-negative and Gram-positive

549 bacteria, *J. Photochem. Photobiol. B: Biol*., 32, 159–164.
550 Miyazaki, Y., Nakashima, T., Iwashita, T., Fujita, T., Yamaguchi, K., Oda, T., 2005.
551 Purification and characterization of photosensitizing hemolytic toxin from
552 harmful red tide phytoplankton, *Heterocapsa circularisquama*. *Aquat. Toxicol.*,
553 73, 382–393.
554 Moan, J., Peng, Q., 2003. An outline of the hundred-year history of PDT. *Anticancer*
555 *Res*., 23, 3591–3600.
556 Oda, T., Sato, Y., Kim, D., Muramatsu, T., Matsuyama, Y., Honjo, T., 2001.
557 Hemolytic activity of *Heterocapsa circularisquama* (Dinophyceae) and its
558 possible involvement in shellfish toxicity. *J. Phycol.*, 37, 509–516.
559 Sato, Y., Oda, T., Muramatsu, T, Matsuyama, Y., Honjo, T., 2002. Photosensitizing
560 hemolytic toxin in *Heterocapsa circularisquama*, a newly identified harmful red
561 tide dinoflagellate. *Aquat. Toxicol.*, 56, 191–196.
562 Soukos, N.S., Ximenez-Fyvie, L.A., Hamblin, M.R., Socransky, S.S., Hasan, T., 1998.
563 Targeted Antimicrobial Photochemotherapy. *Antimicrob. Agents Chemother.*,
564 42, 2595–2601.
565 Tavares, A., Carvalho, C.M.B., Faustino, M. A., Neves, M.G.P.M.S., Tome, J.P.C.,
566 Tome, A.C., Cavaleiro, J.A.S., Cunha, A., Gomes, N.C.M., Alves, E., Almeida,
567 A., 2010. Antimicrobial photodynamic therapy: study of bacterial recovery
568 viability and potential development of resistance after treatment. *Mar. Drugs*, 8,
569 91-105.
570 Xu, Z., Gao, Y., Meng, S., Yang, B., Pang, L., Wang, C., Liu, T., 2016. Mechanism
571 and *In Vivo* Evaluation: Photodynamic Antibacterial Chemotherapy of
572 Lysine-Porphyrin Conjugate. *Front. Microbiol.*, 7, 1–8.

573 Yamamoto, C., Tanaka, Y., 1990. Two species of harmful red tide plankton increased
574 in Fukuoka Bay. *Bull. Fukuoka Fish. Exp. Stn.*, 16, 43–44.
575 Yamasaki, Y., Nagasoe, S., Matsubara, T., Shikata, T., Shimasaki, Y., Oshima, Y.,
576 Honjo, T., 2007. Allelopathic interactions between the bacillariophyte
577 *Skeletonema costatum* and the raphidophyte *Heterosigma akashiwo*, *Mar. Ecol.*
578 *Prog. Ser.*, 339, 83–92.
579 Yamasaki, Y., Zou, Y., Go, J., Shikata, T., Matsuyama, Y., Nagai, K., Shimasaki, Y.,
580 Yamaguchi, K., Oshima, Y., Oda, T., Honjo, T., 2011. Cell contact-dependent
581 lethal effect of the dinoflagellate *Heterocapsa circularisquama* on
582 phytoplankton-phytoplankton interactions. *J. Sea Res.,* 65(1), 76–83.
583

584 **Figure captions**

585

586 Fig. 1. Purification of antibacterial photosensitising agent from the methanol extract of
587 *Heterocapsa circularisquama*. (A) Elution profile of ethanol extract on a Sephadex
588 LH-20 column (3 x 45 cm) previously equilibrated with methanol. The elution pattern
589 was confirmed by three experiments. (B) Photosensitising antibacterial activity of
590 fractions F1–F6 against *S. aureus*. Each fraction (final 1%) was added to *S. aureus* cell
591 suspension in PBS and incubated at 26°C under light illumination (400 ± 5 μmol m^{-2}
592 s^{-1}). After incubation for 2 h, the CFU of each assay mixture was measured as
593 described in the text. The assay was repeated three times. (C) TLC chromatogram of
594 F1–F6 obtained after gel-filtration. Each sample was applied to TLC, and separated
595 spots on the silica gel thin-layer coated with flourescent indicator were detected under
596 ultra violet irradiation. The analysis was repeated five times. (D) Absorption and
597 fluorescence (inset) spectra of F5.

598

599 Fig. 2. Time- and concentration-dependent antibacterial activities of F5 against *S.*
600 *aureus* and *E. coli*. Various concentrations of F5 were added to *S. aureus* or *E. coli* cell
601 suspension in PBS and incubated at 26°C under light illumination (400 ± 5 μmol m^{-2}
602 s^{-1}). After 0.5 (■), 1 (●), or 2 (▲) h of incubation in *S. aureus*, or 2 (△) h of incubation
603 in *E. coli*, the CFU of each assay mixture was measured as described in the text. Each
604 point represents the mean of triplicate measurements. This assay was repeated three
605 times. Each bar represents standard deviation.

606

607 Fig. 3. Photosensitising antibacterial activities of F5 (A) and

608 5,10,15,20-tetra(*N*,*N*,*N*-trimethylanilinium)porphyrin tetratosylate (TPT) (B) against *E.*
609 *coli* (●), *S. aureus* (■), *B. subtilis* (▲), *P. aeruginosa* (◆), and *V. alginolyticus* (×).
610 Various concentrations of F5 or TPT were added to the cell suspension of each strain in
611 PBS and incubated at 26°C under light illumination (400 ± 5 μmol m^{-2} s^{-1}). After
612 incubation for 2 h, the CFU of each assay mixture was measured as described in the
613 text. Each point represents the mean of triplicate measurements. This assay was
614 repeated three times. Each bar represents standard deviation. Inset shows the results of
615 antibacterial activities of F5 against *E. coli* and *V. alginolyticus* at expanded levels of
616 colony forming unit (CFU).
617
618 Fig. 4. Survival rates of *S. aureus* treated with F5 or
619 5,10,15,20-tetra(*N*,*N*,*N*-trimethylanilinium)porphyrin tetratosylate (TPT) for 2 and 8 h
620 without light illumination. F5 or TPT at final concentration of 20 μg mL^{-1} was added to
621 *S. aureus* cell suspension in PBS and incubated at 26°C in the dark. After 2 (□) or 8 (■)
622 h of incubation, the CFU of each assay mixture was measured as described in the text.
623 Each point represents the mean of triplicate measurements. This assay was repeated
624 three times. Each bar represents standard deviation.
625
626 Fig. 5. Electron microscopic observation of *S. aureus* and *E. coli* cells treated with 2 μg
627 mL^{-1} of F5 in the light (400 ± 5 μmol m^{-2} s^{-1}) or in the dark for 2 h. Representative
628 TEM images are shown. (A) *E. coli* untreated control, (B) *S. aureus* untreated control,
629 (C) *E. coli* treated with F5 in the
630 dark, (D) *S. aureus* treated with F5 in the dark, (E) *E. coli* treated with F5 in the light

631 (200 ± 5 μmol m^{-2} s^{-1}), (F) *S. aureus* treated with F5 in the light. The bars indicate 1
632 μm. This observation was repeated two times.
633
634 Fig. 6. Release of intracellular macromolecules from *S. aureus* or *E. coli* treated with
635 F5 in the light (□) or in the dark (■). Bacterial cells were incubated with F5 (final
636 concentration 2 μg mL^{-1}) for 2 h at 26°C in the dark or in the light (400 ± 5 μmol m^{-2}
637 s^{-1}). An aliquot of each reaction mixture was withdrawn and centrifuged (15,000 × *g*
638 for 10 min at 4°C), and then the absorbance of the supernatant at 260 nm was measured.
639 The values are the mean of triplicate measurements. This assay was repeated three
640 times. The bars represent standard deviation. Asterisks denote significant differences (p
641 < 0.05).
642
643 Fig. 7. Binding of F5 to *S. aureus* (●) or *E. coli* (○) cells. (A) Each bacterial cell
644 suspension (5×10^8 CFU mL^{-1}) in PBS was incubated with F5 at a final concentration
645 of 2.2 μg mL^{-1} at 26°C in the dark. After the indicated periods of time, aliquots of the
646 assay mixture were withdrawn and immediately centrifuged (15,000 × *g* for 10 min at
647 4°C). The amounts of unbound F5 in the supernatants were estimated based on the
648 intrinsic fluorescence of F5. Asterisks denote significant differences between *S. aureus*
649 and *E. coli* at 30 min (p < 0.05). (B) Meanwhile, the pelleted cells obtained after 60
650 min incubation were washed once with PBS by centrifugation, resuspended in PBS
651 containing 2% of SDS, and centrifuged (15,000 × *g* for 10 min at 4°C). The amount of
652 F5 released into the supernatants was estimated as described above (□). The pelleted
653 cells were also resuspended in DMSO and sonicated. The amounts of
654 DMSO-extractable F5 were estimated as described above (■). Each point represents

655 the mean of triplicate measurements. Each bar represents standard deviation. This
656 assay was repeated three times. Asterisks denote significant differences between SDS
657 and DMSO extractable F5 levels ($p < 0.05$).
658
659 Fig. 8. Measurement of single oxygen in a solution of F5 in PBS in the light (400 ± 5
660 μmol m^{-2} s^{-1}) (○) or in the dark (●) at 26°C. After incubation for the indicated periods
661 of time, the absorbance of each reaction mixture at 355 nm was measured. (△)
662 absorbance in the light in the presence of 20 mM histidine. This assay was repeated
663 three times.
664
665 Fig. 9. Effect of histidine on the photosensitising antibacterial activity of F5 on *S.*
666 *aureus*. After incubation for 2 h at 26°C in the light (400 ± 5 μmol m^{-2} s^{-1}) in the
667 presence of the indicated concentrations of histidine, the CFU of each assay mixture
668 was measured as described in the text. The values are the mean of triplicate
669 measurements. The bars represent standard deviation. Asterisks denote significant
670 differences ($p < 0.05$). This assay was repeated three times.
671

Fig. 1A

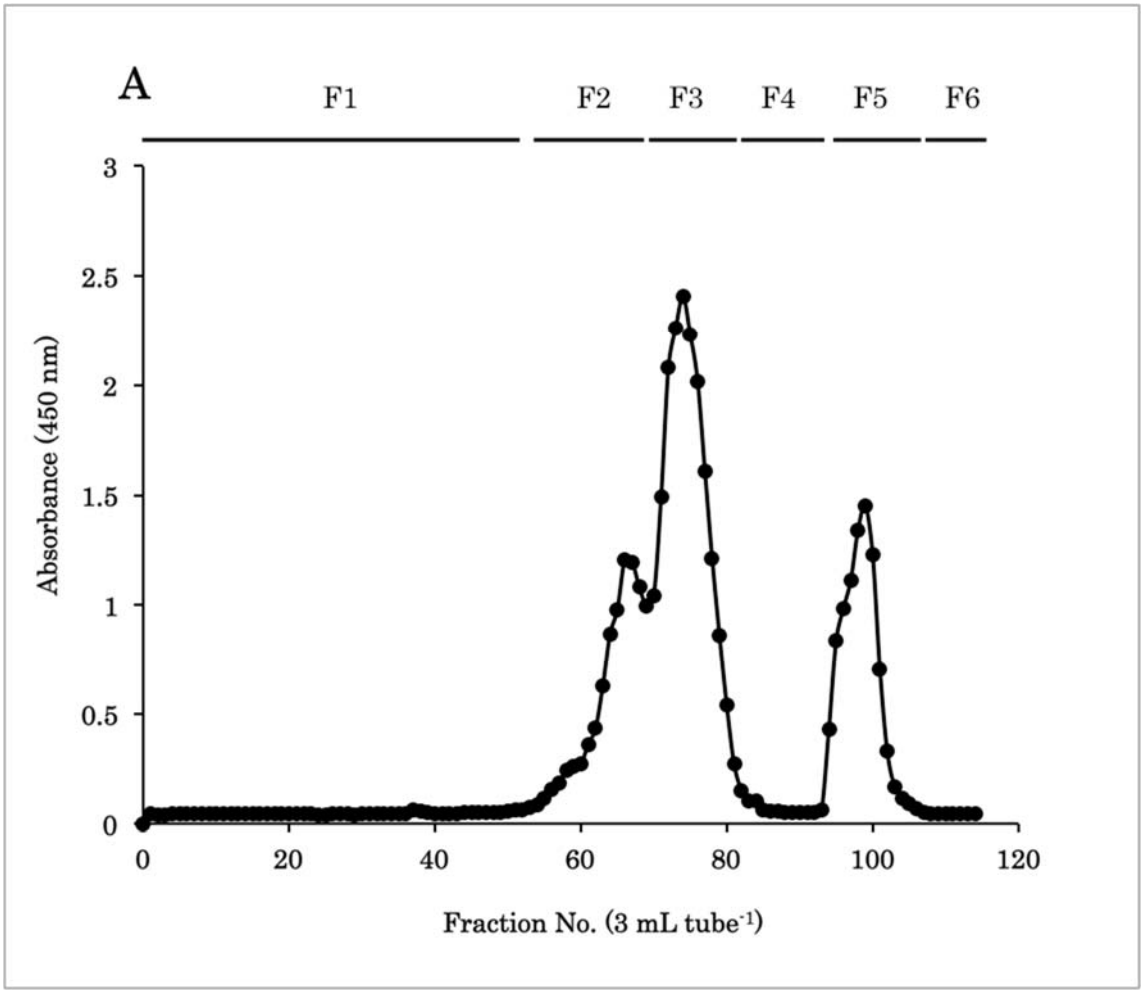
A
F1
F2
F3
F4
F5
F6
Absorbance (450 nm)
3
2.5
2
1.5
1
0.5
0
0
20
40
60
80
100
120
Fraction No. (3 mL tube-1)

Fig. 1B

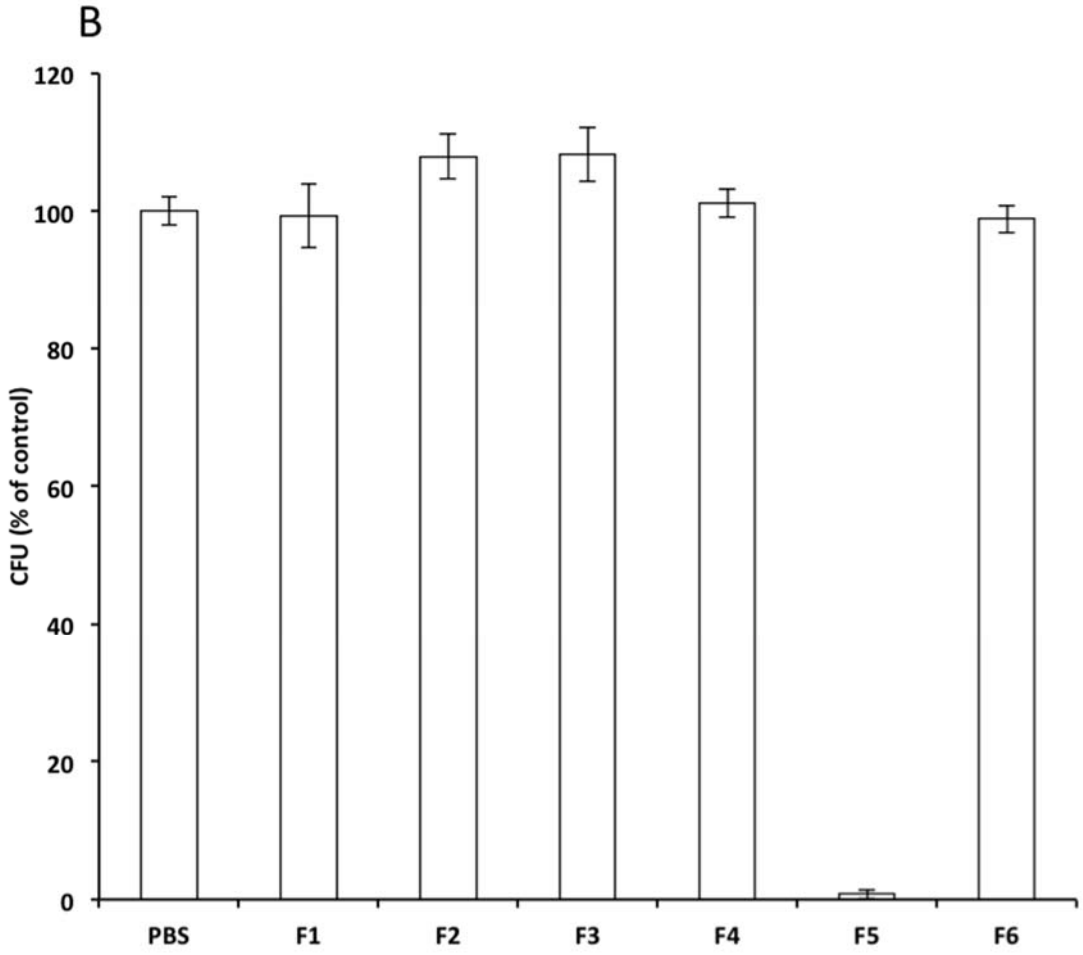

Fig. 1C

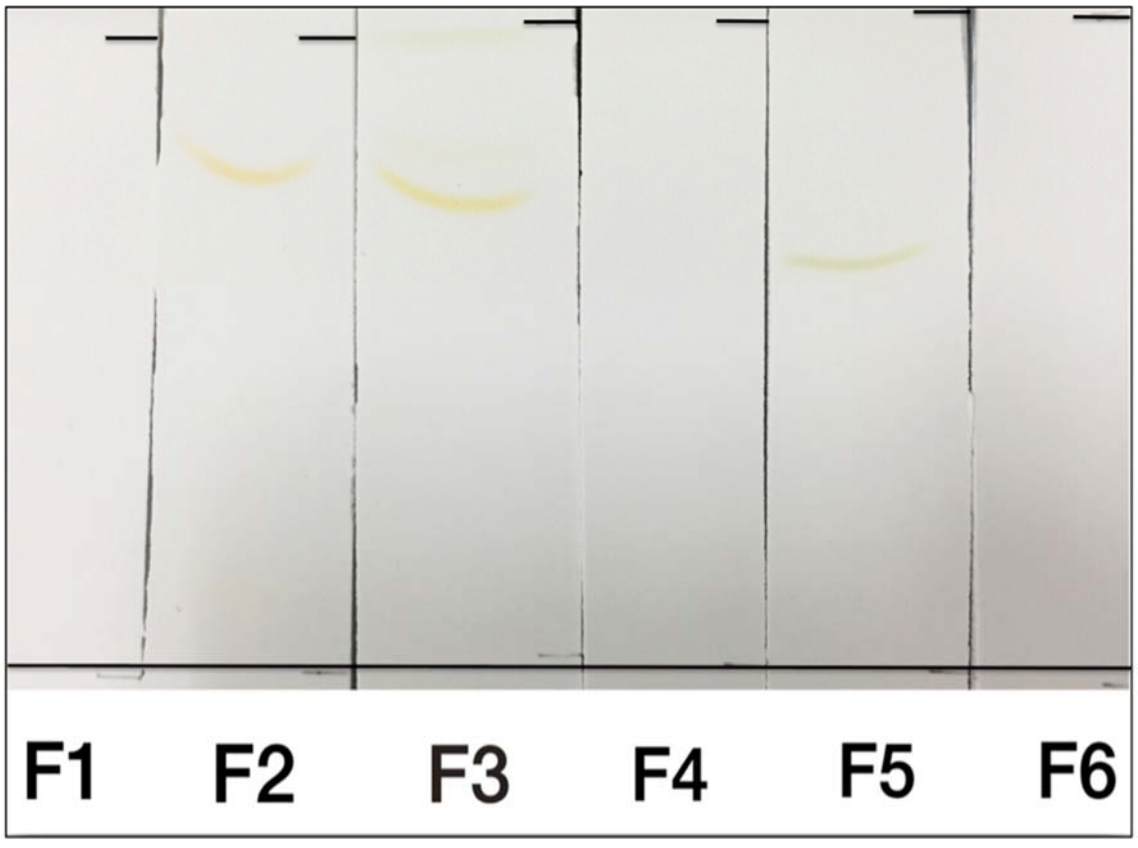

Fig. 1D

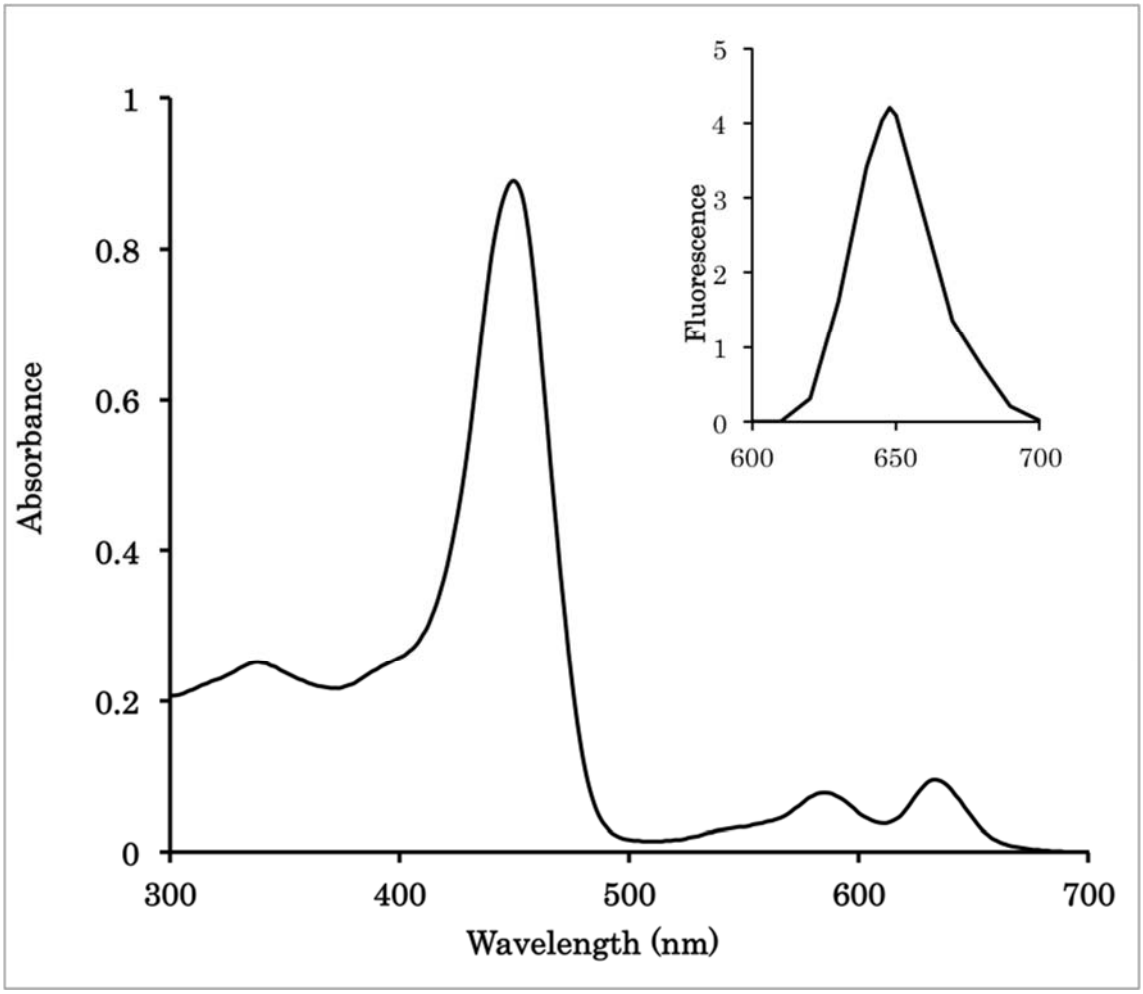
Absorbance
1
0.8
0.6
0.4
0.2
0
300
400
500
600
700
Wavelength (nm)
Fluorescence
5
4
3
2
1
0
600
650
700

Fig. 2

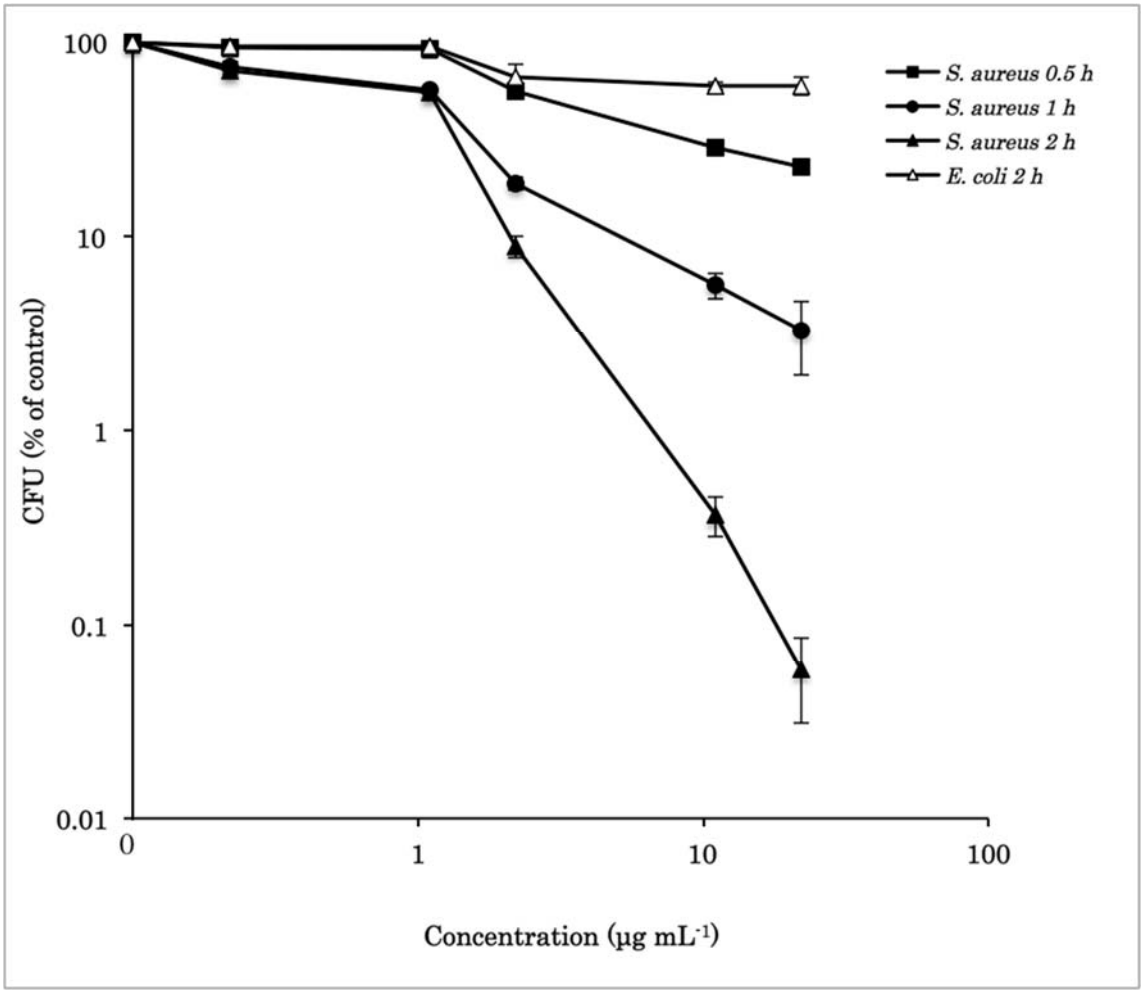
100
10
1
0.1
0.01
CFU (% of control)
0
1
10
100
Concentration (μg mL-1)
S. aureus 0.5 h
S. aureus 1 h
S. aureus 2 h
E. coli 2 h

Fig. 3A

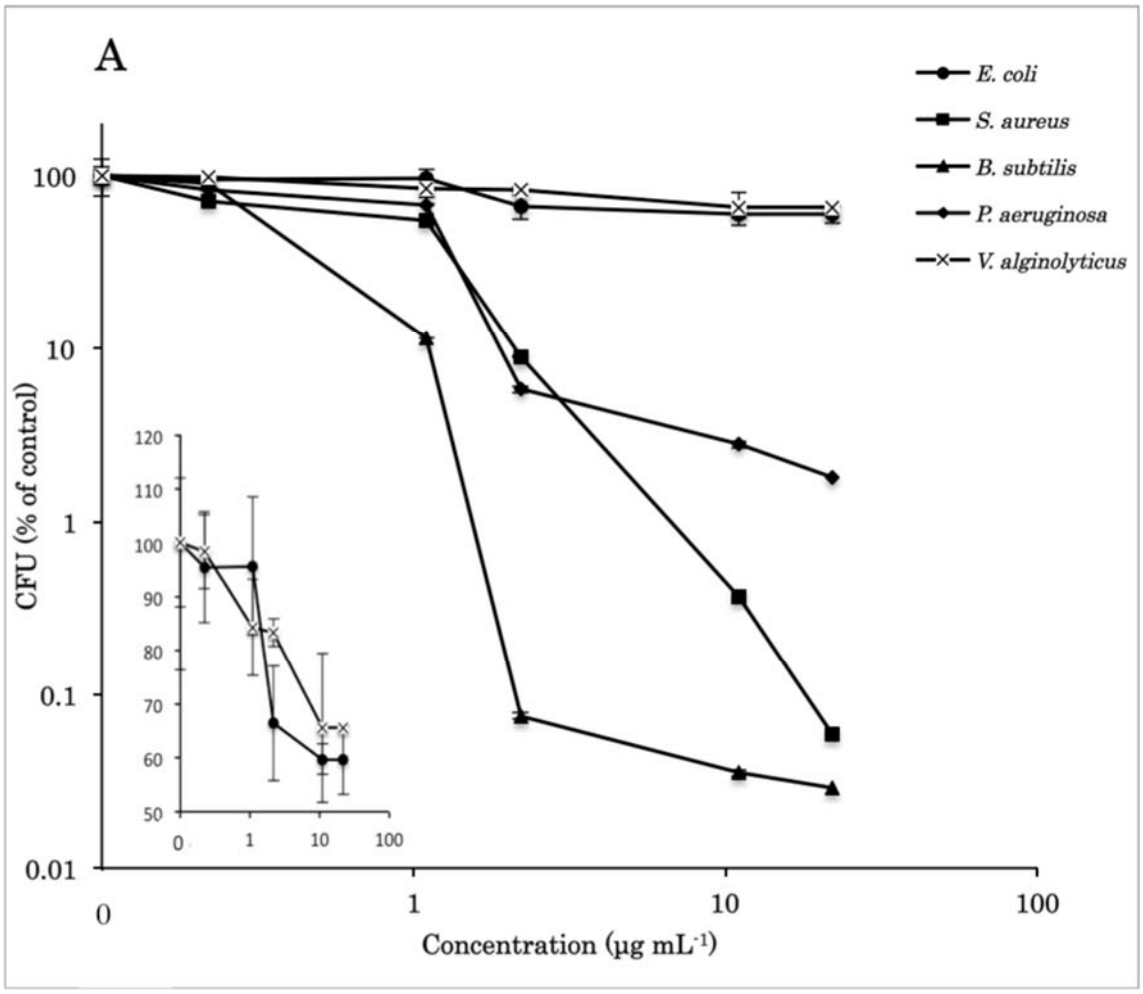
A
E. coli
S. aureus
B. subtilis
P. aeruginosa
V. alginolyticus
CFU (% of control)
100
10
1
0.1
0.01
0
1
10
100
Concentration (μg mL-1)
120
110
100
90
80
70
60
50
0
1
10
100

Fig. 3B

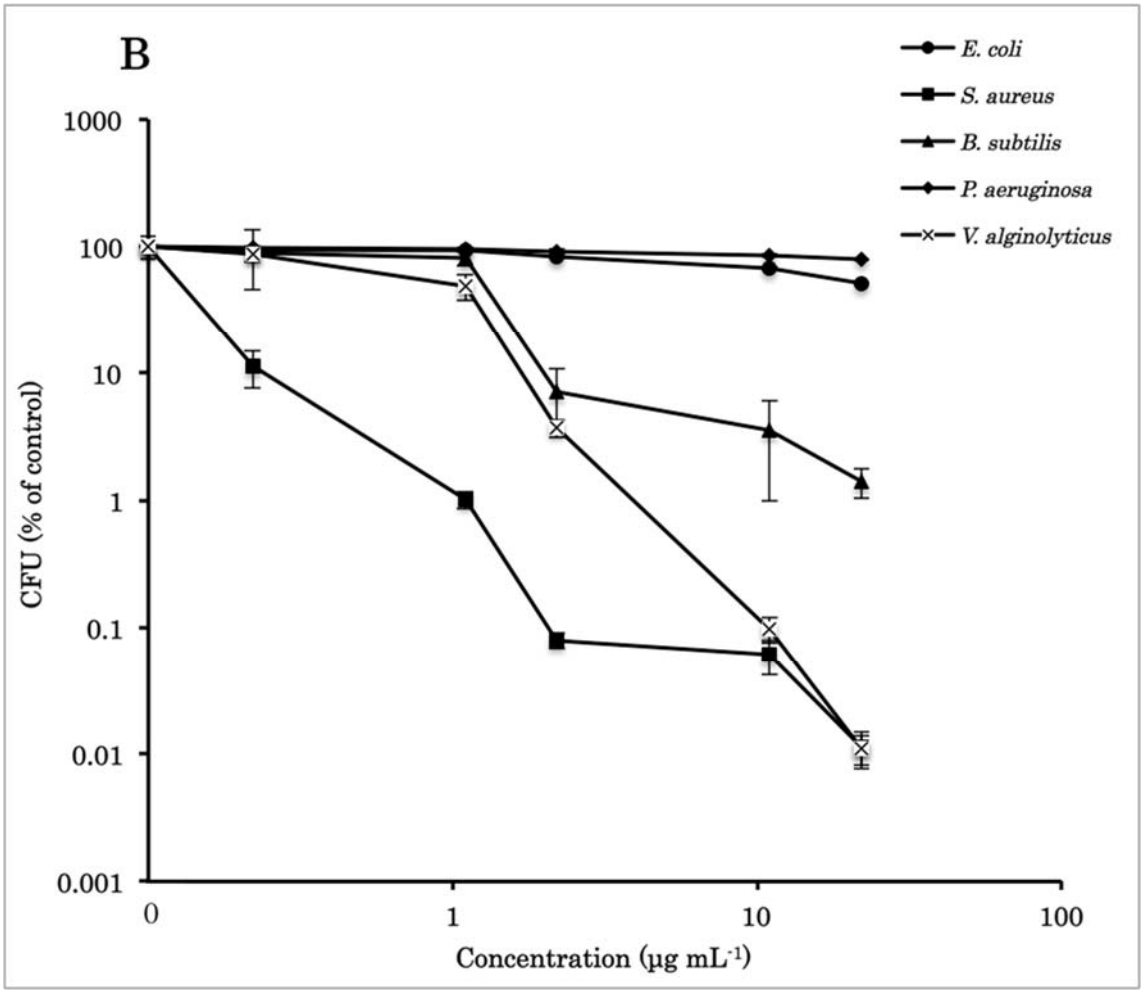
B
E. coli
S. aureus
B. subtilis
P. aeruginosa
V. alginolyticus
1000
100
10
1
0.1
0.01
0.001
CFU (% of control)
0
1
10
100
Concentration (μg mL-1)

Fig. 4

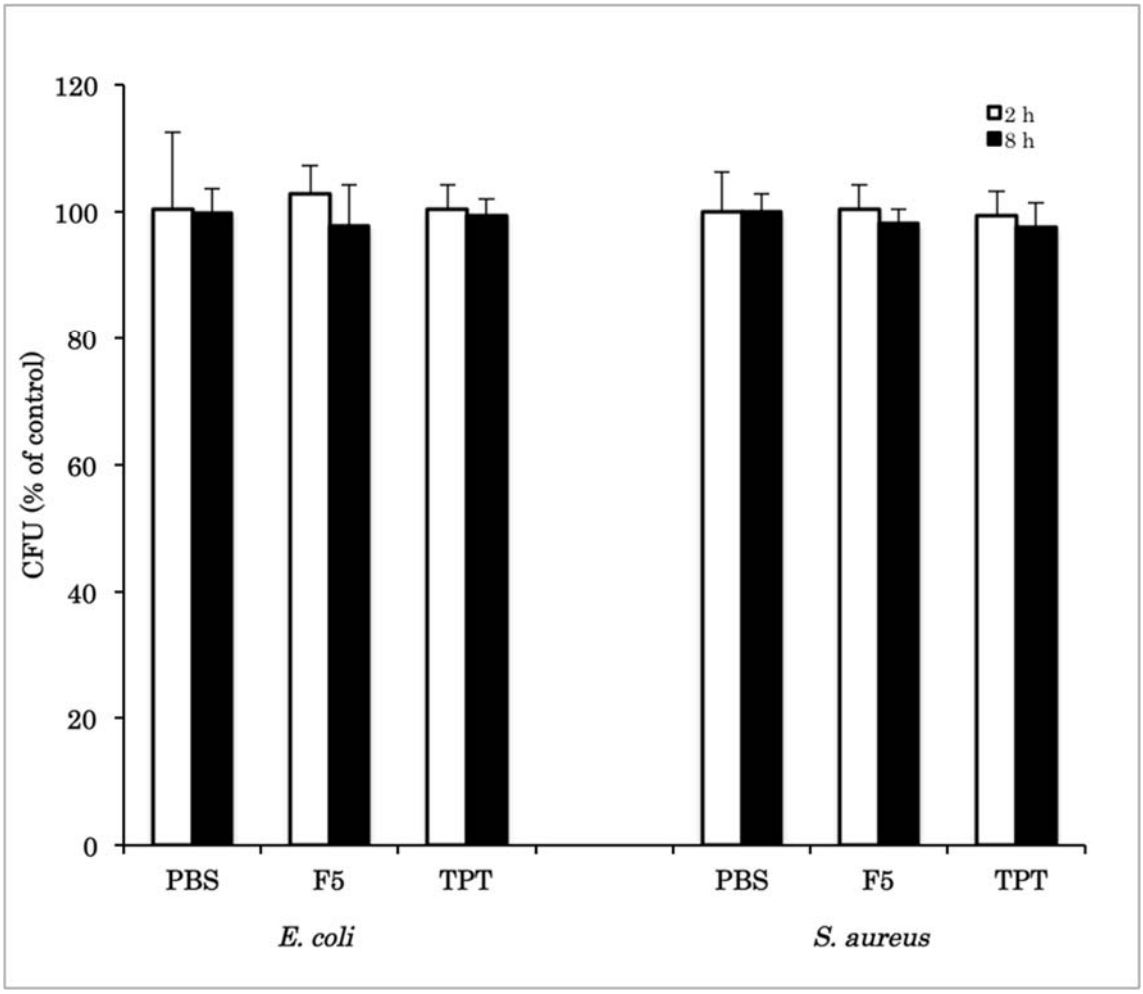
120
100
80
60
40
20
0
CFU (% of control)
2 h
8 h
PBS
F5
TPT
PBS
F5
TPT
E. coli
S. aureus

Fig. 5

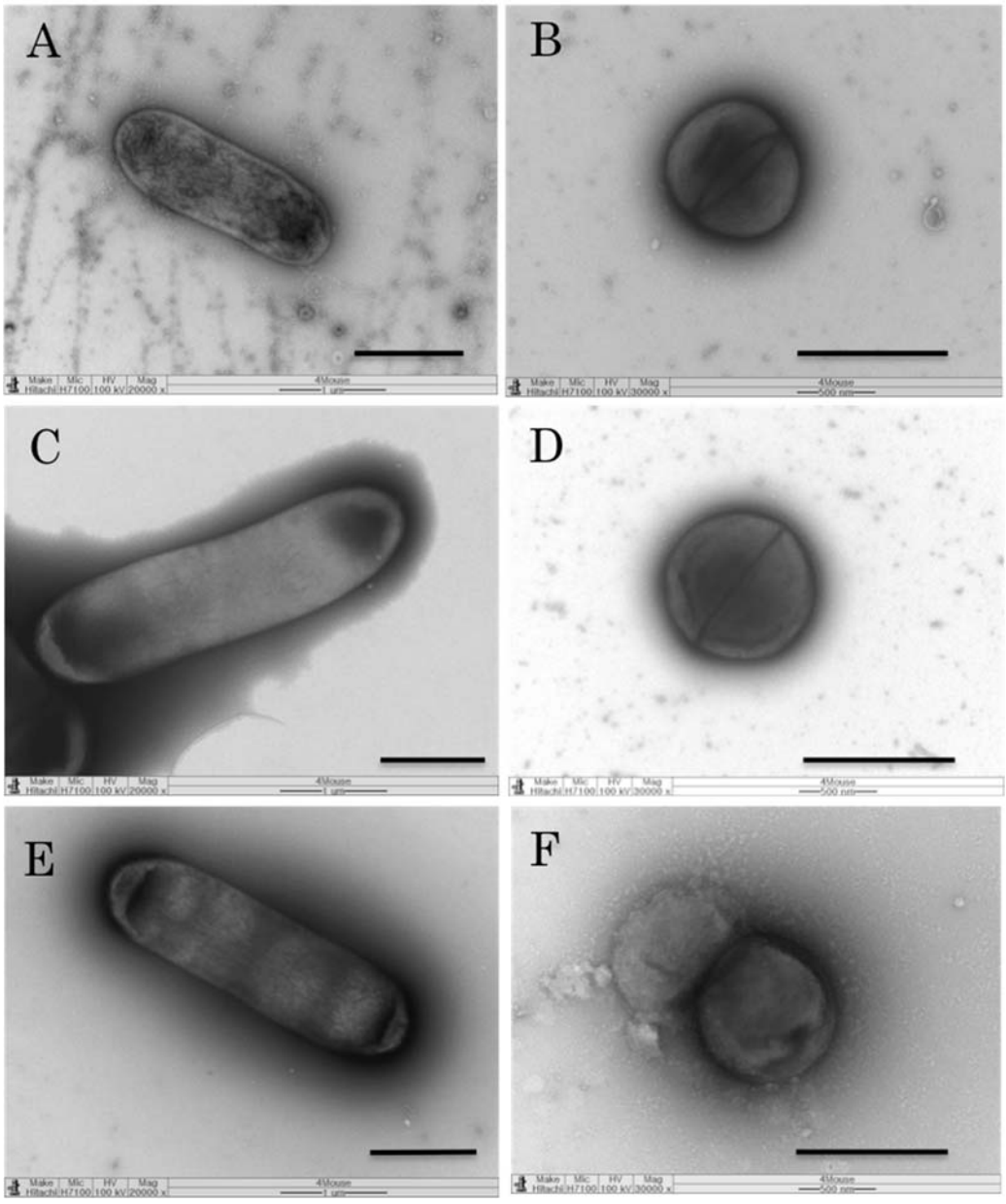

Fig.6

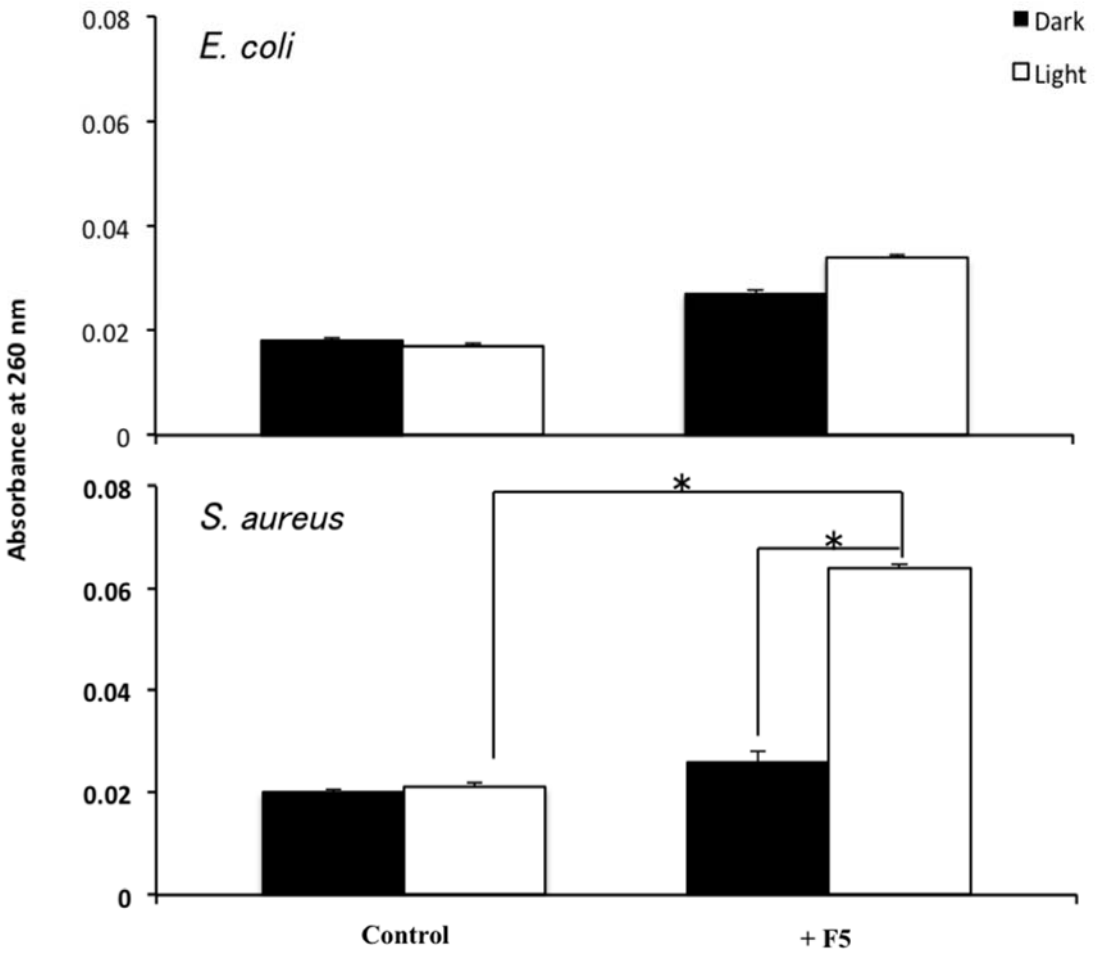
E. coli
S. aureus
Dark
Light
Absorbance at 260 nm
0.08
0.06
0.04
0.02
0
*
*
Control
+ F5

Fig. 7A

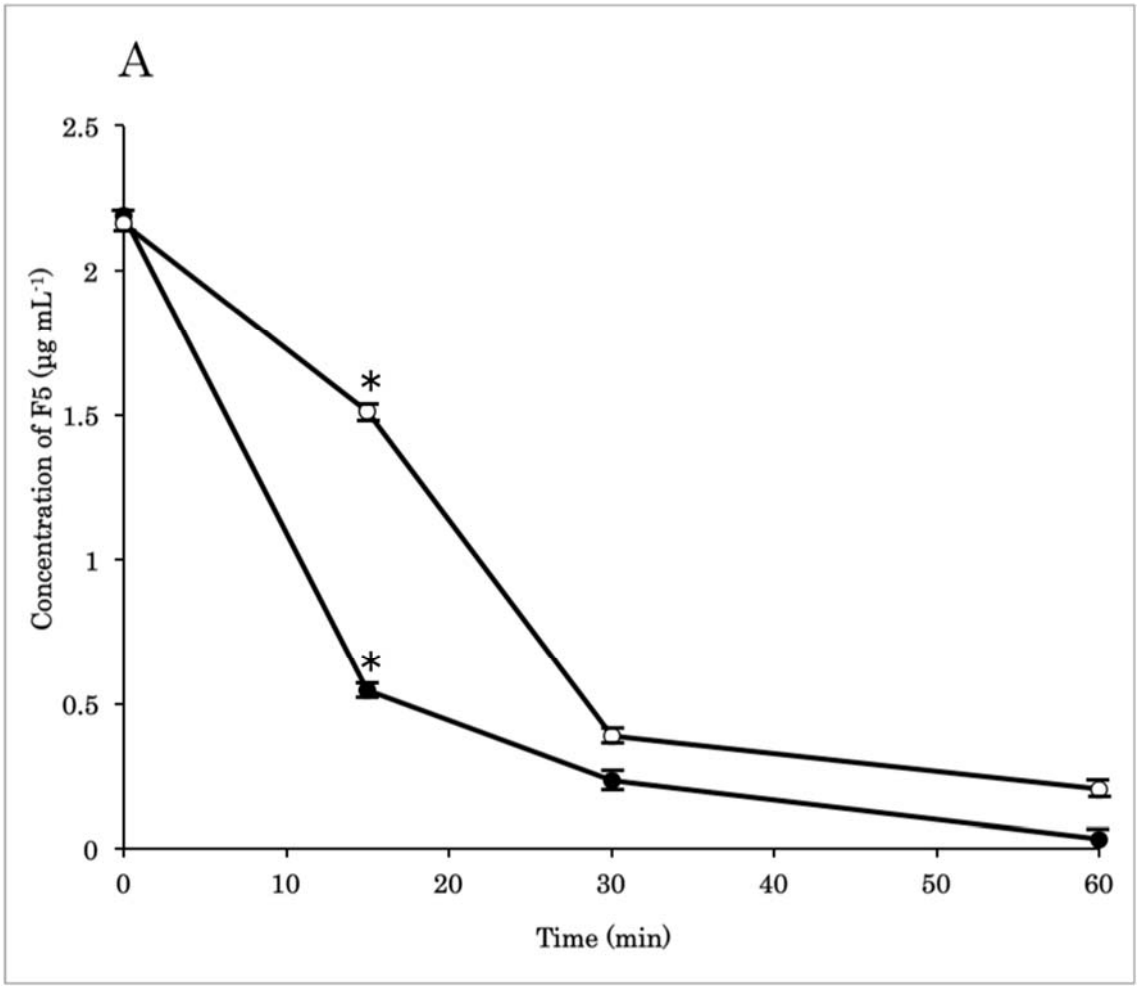
A
2.5
2
1.5
1
0.5
0
Concentration of F5 (μg mL-1)
*
*
0
10
20
30
40
50
60
Time (min)

Fig. 7B

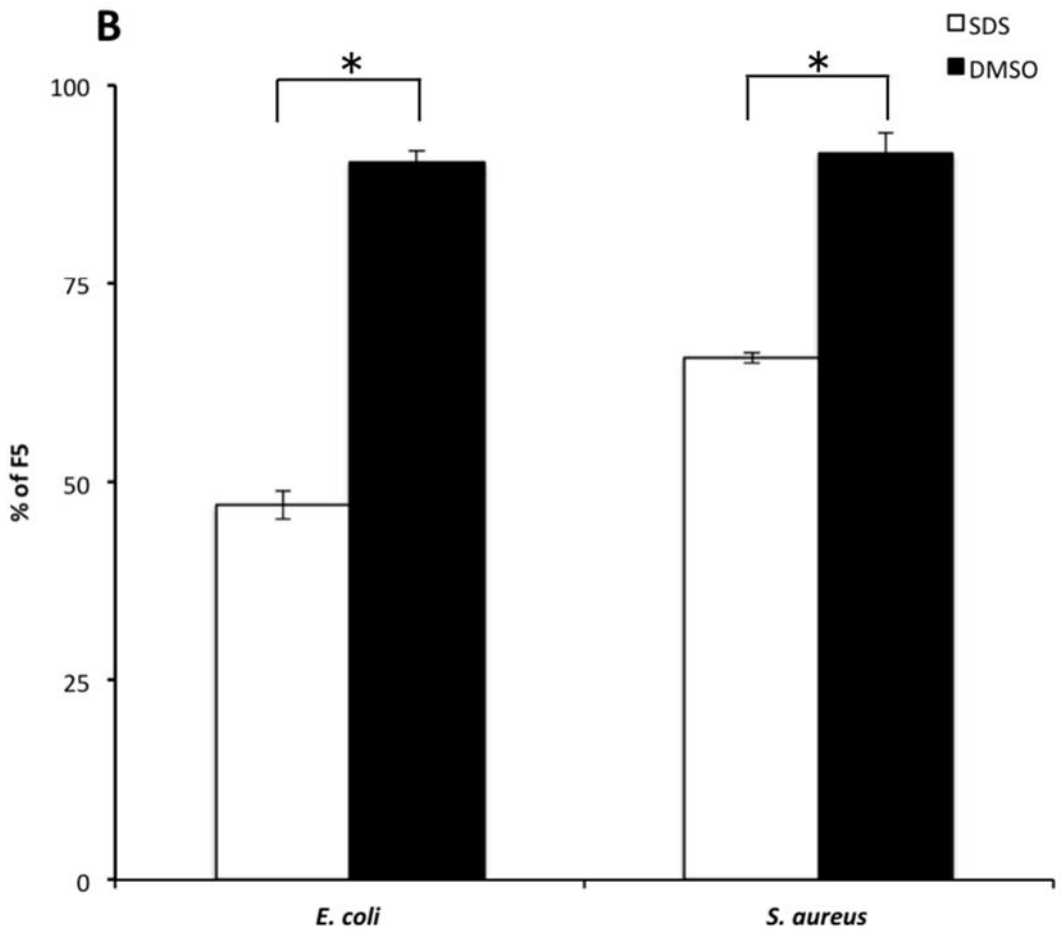

Fig. 8

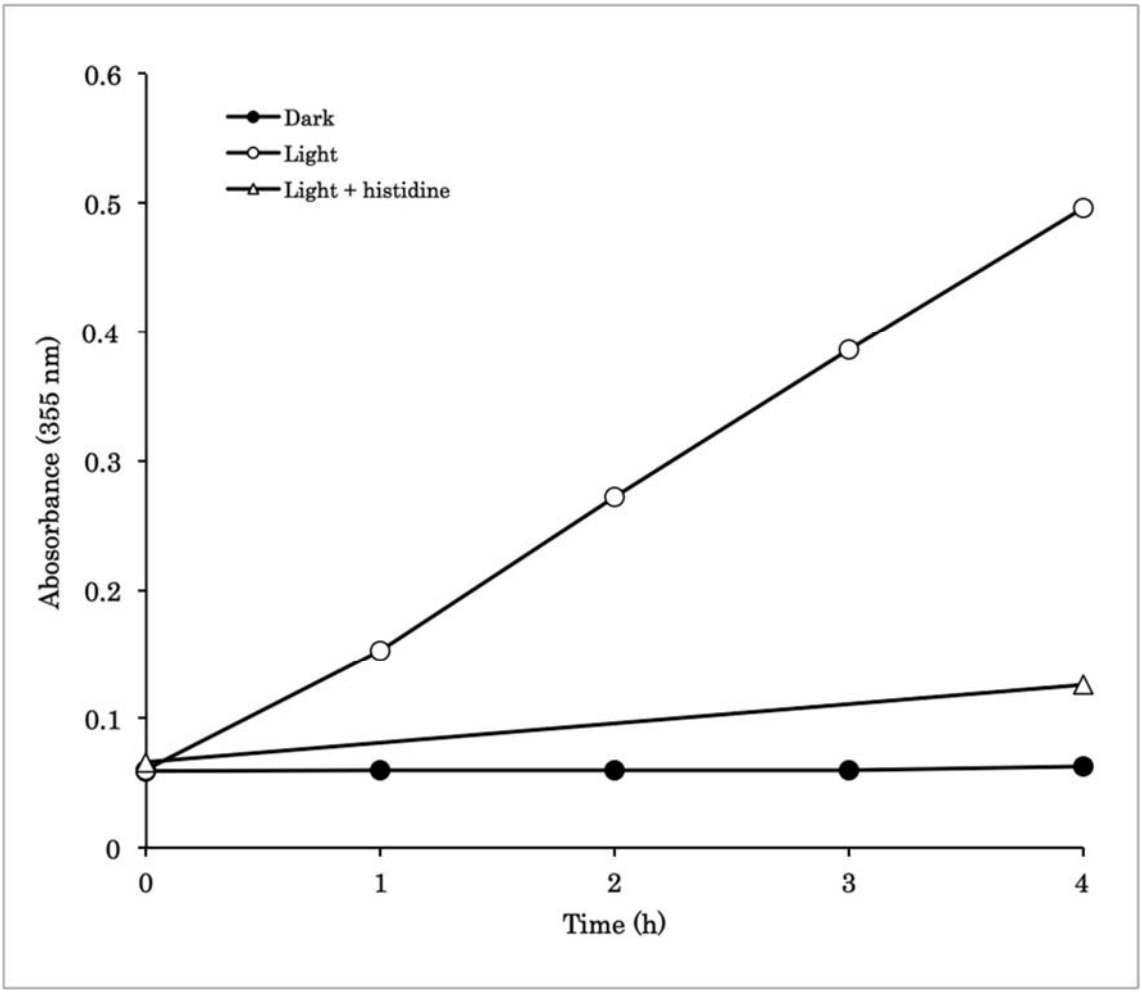
Dark
Light
Light + histidine
Abosorbance (355 nm)
0.6
0.5
0.4
0.3
0.2
0.1
0
0
1
2
3
4
Time (h)

Fig. 9

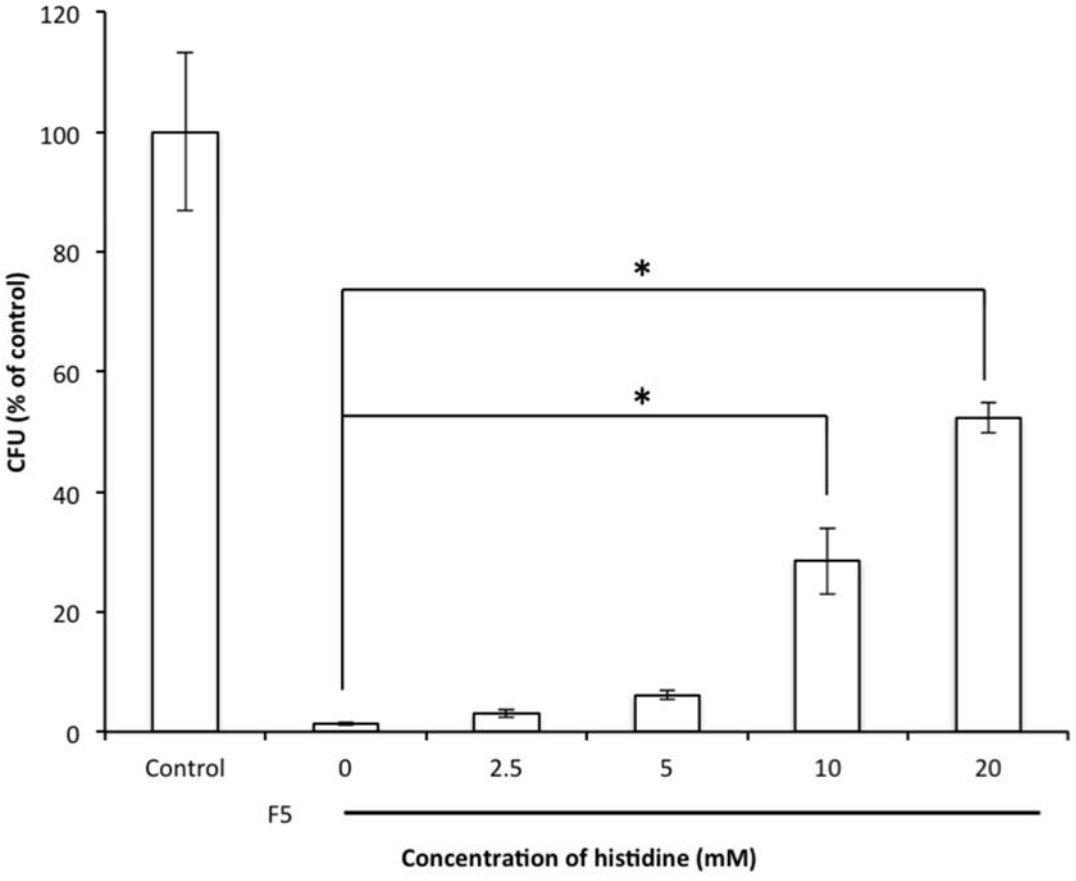
120
100
80
60
40
20
0
CFU (% of control)
*
*
Control
0
2.5
5
10
20
F5
Concentration of histidine (mM)